

IMPACT TOUGHNESS BEHAVIOUR OF A516 GR. 60 STEEL WELDED JOINTS

UDARNA ŽILAVOST ZAVARENIH SPOJEVA ČELIKA A516 GR. 60

Originalni naučni rad / Original scientific paper

Rad primljen / Paper received: 27.08.2024

<https://doi.org/10.69644/ivk-2024-02-0232>

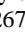
Adresa autora / Author's address:

¹⁾ University of Kosovska Mitrovica, Faculty of Technical Sciences, Serbia I. Čamagić  0000-0003-4706-6333

²⁾ University of Belgrade, Faculty of Mechanical Eng., Serbia

email: aleksandarsedmak@gmail.com  0000-0002-5438-1895

³⁾ Military Technical Institute, Belgrade, Serbia

⁴⁾ Innovation Center of the Faculty of Mechanical Engineering, Belgrade, Serbia  0000-0002-2674-541X

⁵⁾ Serbian Committee for Energy Network, Belgrade, Serbia

⁶⁾ Naftagas - Tehnički servisi d.o.o., Pančevo, Serbia

Keywords

- A516 Gr. 60
- impact toughness
- total impact energy
- welded joint zones

Abstract

Impact fracture behaviour of welded joints made of A516 Gr. 60 is analysed as a commonly used carbon structural steel for welded structures. Impact testing on Charpy instrumented pendulum is performed using specimens with a notch at positions: base metal (BM), heat-affected-zone (HAZ), and weld metal (WM). The total impact energy is presented as a sum of energies for crack initiation and crack propagation to make the analysis more sophisticated and comprehensive. The effect of temperature up to -60 °C was also analysed to prove the A516 Gr. 60 steel usability at subzero conditions.

INTRODUCTION

Before using welded joints made of A516 Gr. 60 steel, it is necessary to investigate their properties, with the focus on impact toughness and microstructure to ensure operational safety. Each welded joint region (BM, WM and HAZ) has to be analysed individually, and their impact toughness and transition temperatures determined and compared to each other, to account for the heterogeneity of a weld, /1-3/. Crack initiation energy and crack propagation energy, as components of total impact energy should also be considered separately, to provide insight into the nature of fracture which occurred under the effect of impact load at lower temperatures. The main issue here is transition temperature, as a phenomenon which is decisive for the use of a material at lower temperature, as described before in a couple of recent papers, /4-7/.

Ključne reči

- A516 Gr. 60
- udarna žilavost
- ukupna udarna energija
- zone zavarenog spoja

Izvod

Analizirano je ponašanje zavarenih spojeva od konstrukcionog čelika A516 Gr. 60 pri lomu usled udarnog opterećenja. Udarno ispitivanje je urađeno na instrumentiranom Šarpijevom klatnu, na epruvetama sa zarezom u osnovnom metalu (OM), zoni uticaja toplote (ZUT) i metalu šava (MŠ). Ukupna udarna energija je predstavljena kao suma energije nastajanja prsline i energije rasta prsline, kako bi ova analiza bila detaljnija i sveobuhvatnija. Uticaj temperature do -60 °C je takođe analiziran, kako bi se potvrdilo da je čelik A516 Gr. 60 upotrebljiv i na niskim temperaturama.

MATERIAL AND WELDING PLAN

The A516 Gr.60 is a low-alloyed carbon steel, used mainly for pressure vessels, such as spherical tanks and tanks for gas storage. This is largely due to its exceptional mechanical properties at lower temperatures. Its minimum yield stress is 255 MPa and its guaranteed toughness at -40 °C is 41 J. It was manufactured in 'Železarna ACRONI', Jesenice, /8-9/. Plates with a thickness of 15 mm were available for experimental tests. The chemical composition of steel A516 Gr. 60 is shown in Table 1.

Test specimens are made out of welded joints produced using manual arc welding (MAW) process, with EVB Ni electrode as filler material. Nominal mechanical properties and chemical composition for the filler material are shown in Tables 2 and 3.

Table 1. Chemical composition of the tested batch of steel A516 Gr. 60, Batch no. 191314030402, /8/.

Measuring number	Element, % wt.										
	C	Si	Mn	P	S	Cu	Al	Cr	Mo	Ni	N
1	0.18	0.19	0.86	0.009	<0,001	0.24	0.036	0.12	0.05	0.16	0.007
2	0.17	0.20	0.86	0.005	<0,001	0.24	0.037	0.12	0.05	0.15	0.004
3	0.19	0.20	0.88	0.007	<0,001	0.25	0.041	0.12	0.05	0.15	0.005
Mean value	0.18	0.20	0.86	0.007	<0,001	0.24	0.038	0.12	0.05	0.15	0.005

Table 2. Chemical composition of filler metal EVB Ni.

Filler material	% wt.						
	C	Si	Mn	Ni	P	S	N
EVB Ni	0.07	0.50	1.40	1.1	0.009	0.011	0.012

Table 3. Mechanical properties of filler material EVB Ni.

Yield stress R _{p0.2} (MPa) min	Tensile strength R _m (MPa)	Elongation A, %, min.	Impact energy KV (J) at -40°C, min.
460	560-720	22	47

Welding plan was defined as follows: root pass - MAW process (denoted as 111 according to EN ISO standards). Filler material was EVB Ni, with a diameter of 2.5 mm. Fill passes - MAW process for all passes. Same filler material as the root pass, but with diameters of 2.5 and 3.25 mm.

Schematic display of the preparation and weld geometry is shown in Fig. 1, whereas the order of welding passes is shown in Fig. 2.

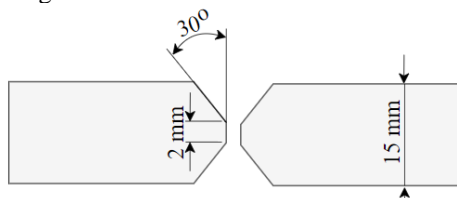


Figure 1. Schematic display of weld geometry and preparation

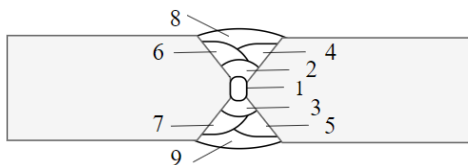


Figure 2. Welding sequence

After the machining of the weld, pre-heating to a temperature of around 120 °C was performed.

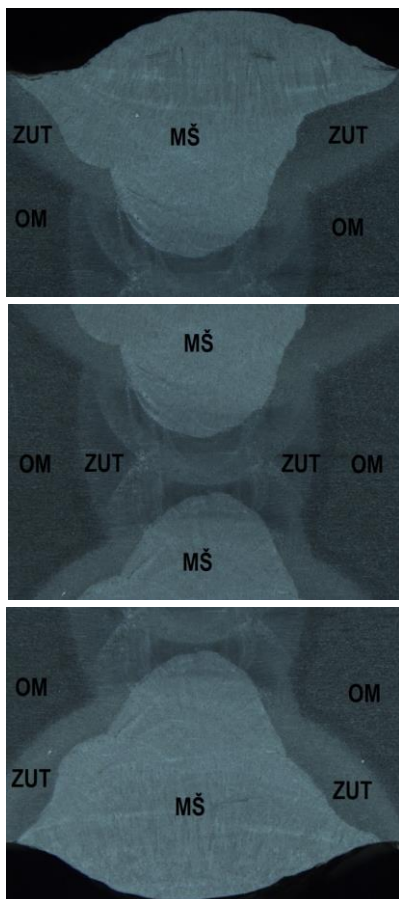


Figure 3. Weld face (top), central section (middle), and root (bottom).

In order to gain a clearer insight into the microstructure of the welded joint, with distinctive regions, images are made using a stereo microscope with magnitude 12. Figure 3

shows the weld face, its central section and weld root. All three regions of the welded joint can be clearly seen in the images: the base metal (BM), heat affected zone with the fusion line (HAZ-FL), and weld metal (WM). Microstructures of BM, HAZ, FL, and WM of the joint are shown in Figs. 4-7.

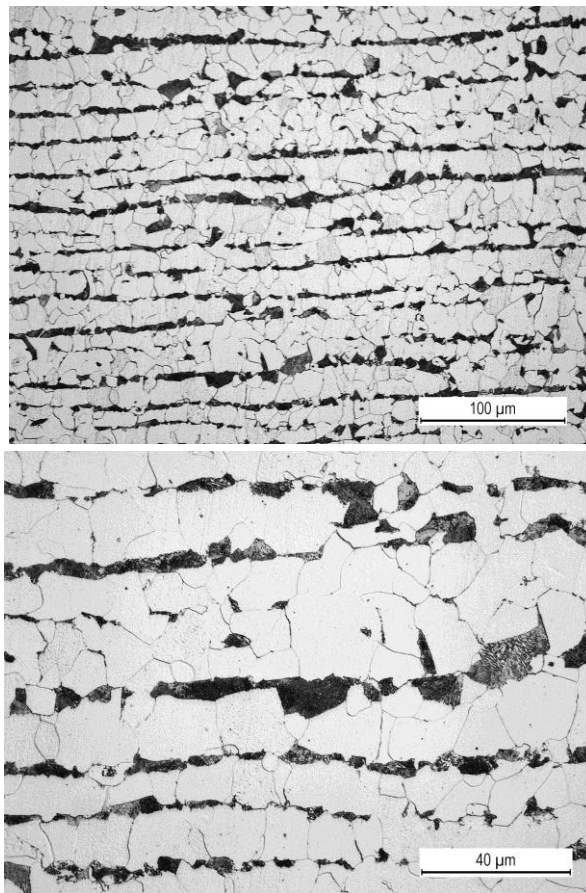
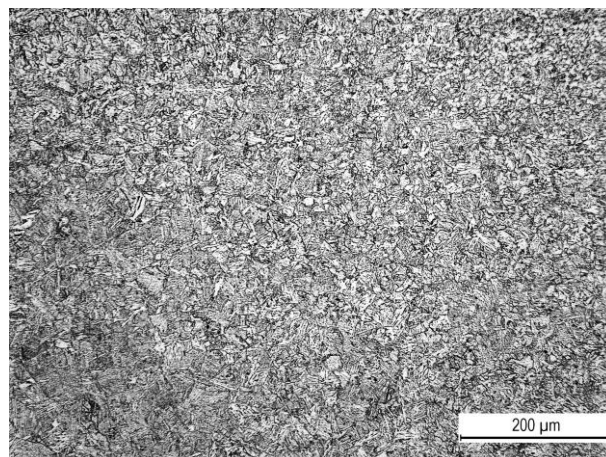


Figure 4. Microstructure of BM (low-alloyed steel A516 Gr. 60).

It can be seen that the BM has a uniformly distributed ferrite-pearlite structure. Ferrite is found in the shape of polygonal crystals, whereas pearlite resembles a compact dark micro-constituent. Weld metal and heat affected zone also have a prominent ferrite-pearlite structure.



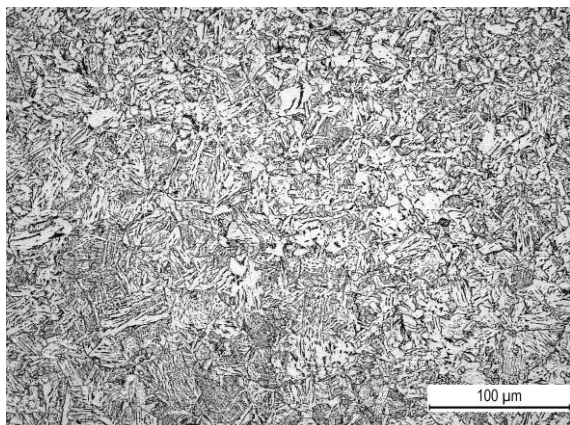


Figure 5. Microstructure of HAZ (low-alloyed steel A516 Gr. 60).

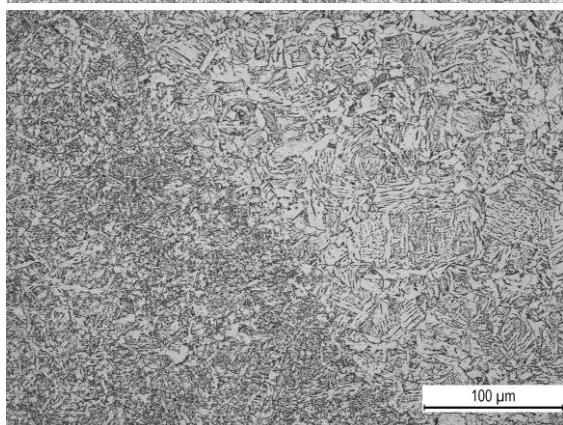
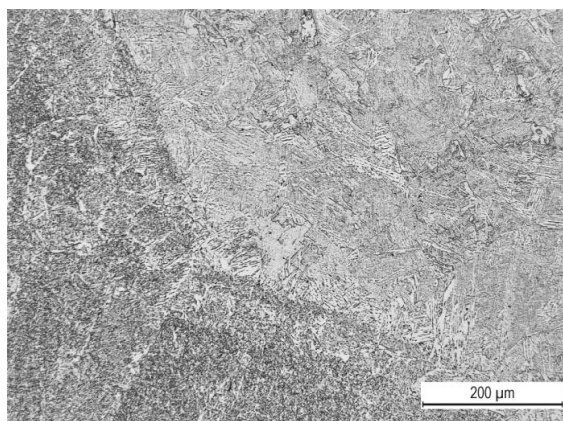


Figure 6. Microstructure of FL (steel A516 Gr. 60).

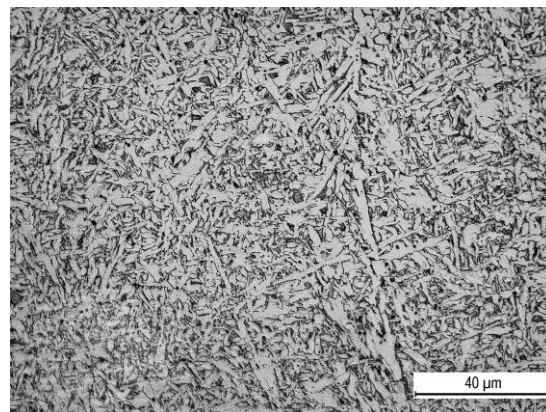
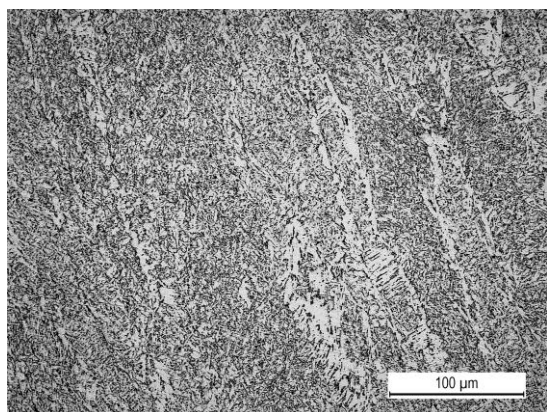


Figure 7. Microstructure of WM (steel A516 Gr. 60).

IMPACT TESTS

Standard Charpy specimens are used for impact tests, /10/, shown in Fig. 8. Three groups of specimens are tested, depending on the location of the V-2 notch: Group I - specimens with a notch in BM, Group II - specimens with notch in the BM, and Group III - specimens with notch in the HAZ. Their geometry is shown in Fig. 9.

In accordance with standard SRPS EN ISO 9016:2022, /11/, specimen type VWT (V: Charpy notch, W: notch in the weld metal, T: notch perpendicular to the thickness) was used for WM, and VHT was used for the HAZ (H refers to the notch in HAZ and other designations are the same as the previous type). The way of positioning the notch in the corresponding welded joint region is shown in Fig. 9, /11/.

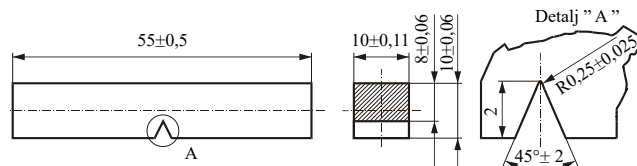


Figure 8. Dimensions of test specimens and the V-2 notch, /11/.

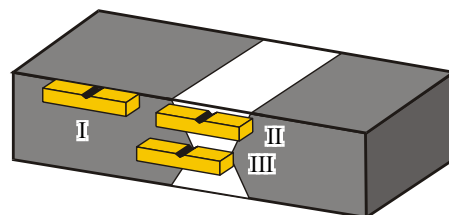


Figure 9. Scheme of notch locations in a welded joint, /11/.

However, since tests were performed using an instrumented Charpy pendulum (in accordance with standard SRPS EN ISO 14556:2023), total impact energy W_t was calculated as the surface area between the force-displacement (deflection) curve and the x axis. The following interpretations and analyses, including tabular and graphic representations of test results are presented in accordance with the aforementioned standard. Force-displacement curves enable the separation of total impact energy (W_t) into the energy for crack initiation (W_i) and energy for crack propagation (W_p), /12-15/. Testing equipment used in this analysis is shown in Fig. 10.



Figure 10. Instrumented Charpy pendulum WOLPERT 150/300J.

IMPACT TEST RESULTS FOR BM, HAZ AND WM

Results of impact testing of specimens with a notch in the BM are given in Table 4. Diagrams force vs. time are shown in Fig. 11 for BM specimens (and different test temperatures). Results of tests performed on specimens with a notch in the HAZ are presented in the same form, in Table 5 and Fig. 12. For specimens with the notch in the WM, results are given in Table 6 and Fig. 13.

Table 4. Values of impact energy the BM.

Specimen designation	Temp. °C	Initiation energy W_i (J)	Propagation energy W_p (J)	Total impact energy W_t (J)
1A	-60	25.5	7.8	33.3
2A		27.5	10.9	38.4
3A		27.1	8.1	35.3
1B	-40	51.3	21.2	72.5
2B		45.1	21.8	66.9
3B		42.4	24.4	68.6
1C	-20	51.3	71.0	122.3
2C		53.9	70.8	124.7
3C		53.9	73.8	127.7
1D	0	62.8	95.4	158.2
2D		64.4	98.6	163.0
3D		60.4	91.1	151.6
1E	20	62.6	139.9	202.5
2E		62	133.4	195.3
3E		65.4	141.7	207.1

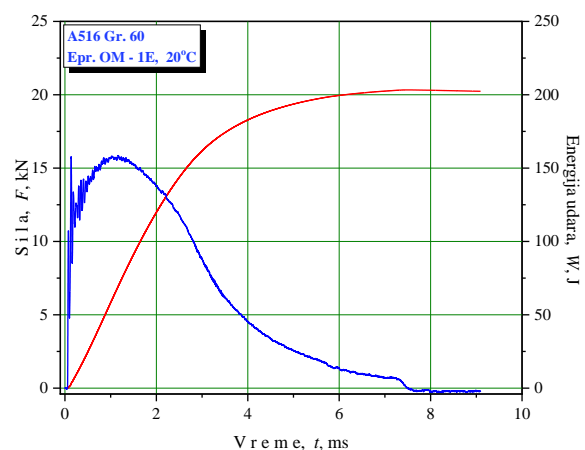
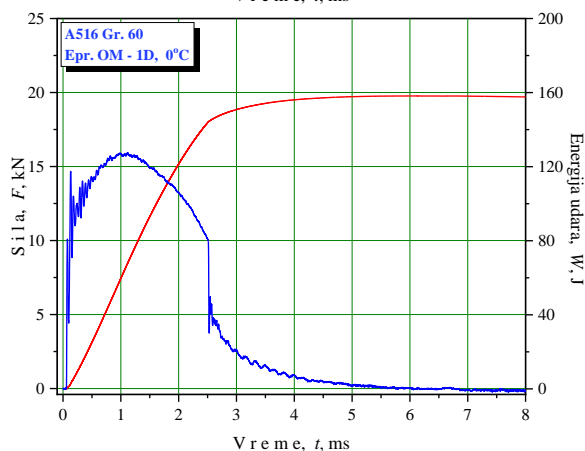
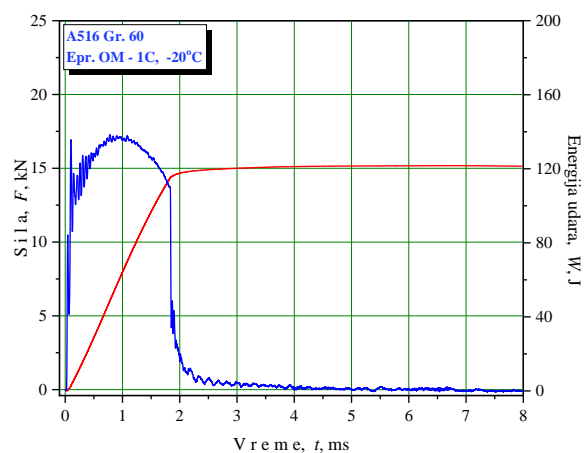
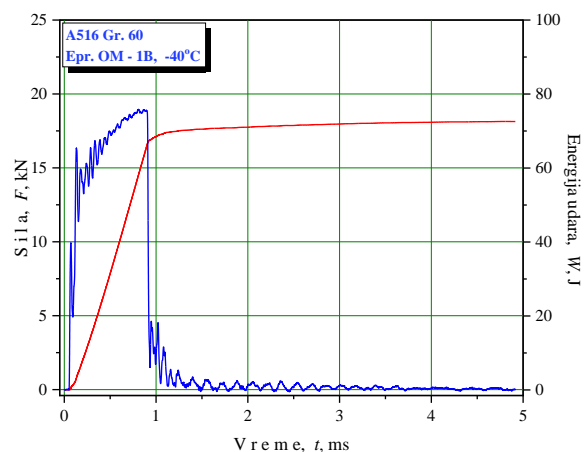
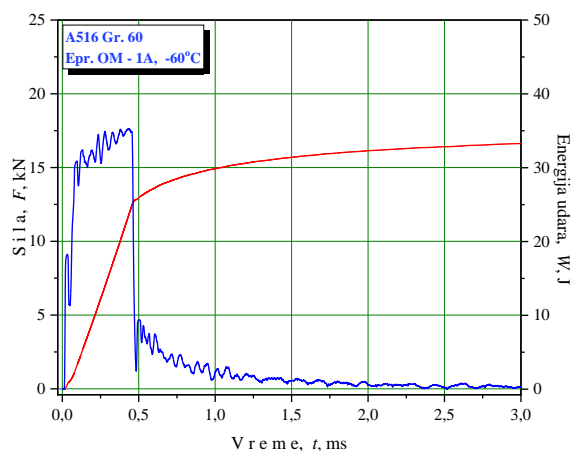


Figure 11. The BM results - force-time diagrams

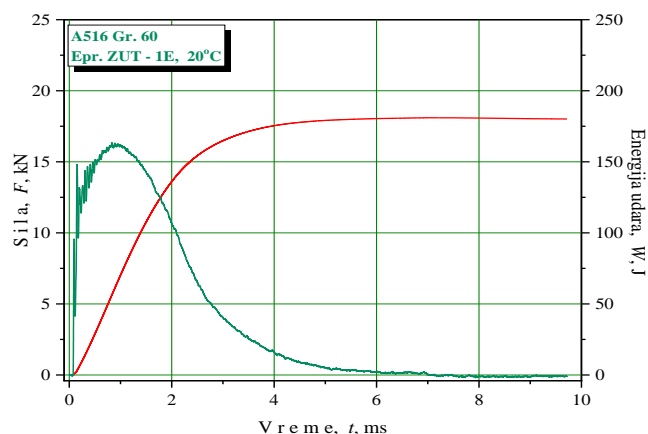
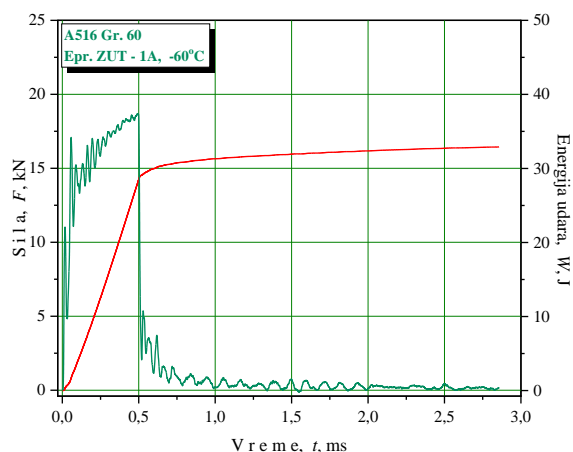


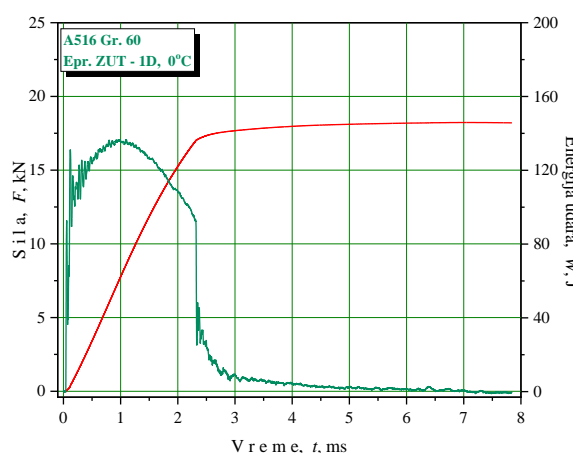
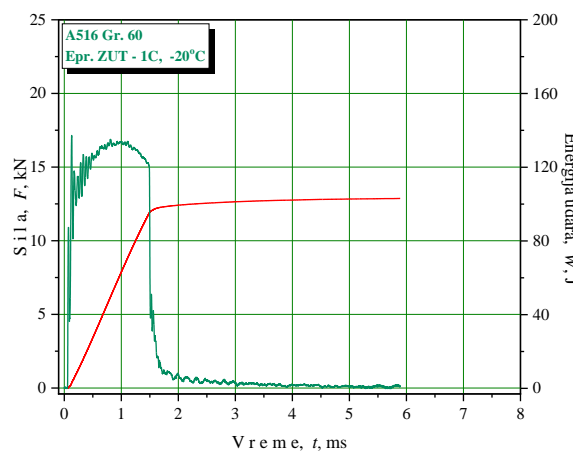
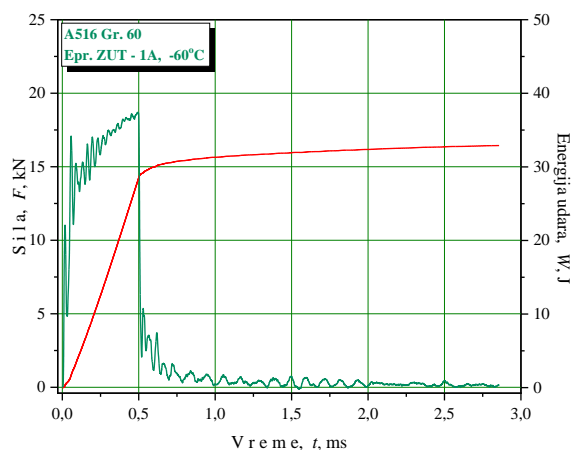
Figure 12. The HAZ results - force-time diagrams.

Table 5. Impact energy for specimens with notch in HAZ

Specimen designation	Temp. °C	Initiation energy W_i (J)	Propagation energy W_p (J)	Total impact energy W_t (J)
ZUT - 1A	-60	28.6	4.3	32.9
ZUT - 2A		26.9	3.5	30.4
ZUT - 3A		28.1	3.4	31.4
ZUT - 1B	-40	45.6	14.3	59.9
ZUT - 2B		41.4	13.8	55.2
ZUT - 3B		47	15.2	62.2
ZUT - 1C	-20	50.3	52.8	103.1
ZUT - 2C		53.7	53.4	107.1
ZUT - 3C		55.6	56.0	111.6
ZUT - 1D	0	59.4	86.5	145.8
ZUT - 2D		60.2	83.4	143.6
ZUT - 3D		60	79.6	139.6
ZUT - 1E	20	57.2	123.0	180.2
ZUT - 2E		60.4	116.5	176.9
ZUT - 3E		61.8	120.4	182.2

Table 6. Values of impact energy for the WM.

Specimen designation	Temp. °C	Initiation energy W_i (J)	Propagation energy W_p (J)	Total impact energy W_t (J)
MŠ - 1A	-60	23.8	5.5	29.3
MŠ - 2A		26.8	3.4	30.2
MŠ - 3A		27.3	1.3	28.6
MŠ - 1B	-40	33.0	11.4	44.4
MŠ - 2B		32.9	10.4	43.3
MŠ - 3B		33.7	12.3	46.0
MŠ - 1C	-20	49.9	37.2	87.1
MŠ - 2C		47.1	30.1	77.2
MŠ - 3C		48.1	34.9	83.0
MŠ - 1D	0	55.6	51.4	107.0
MŠ - 2D		58.9	57.5	116.4
MŠ - 3D		56.7	54.4	111.1
MŠ - 1E	20	65.7	88.9	154.6
MŠ - 2E		62.6	92.7	155.3
MŠ - 3E		65.4	92.2	157.6



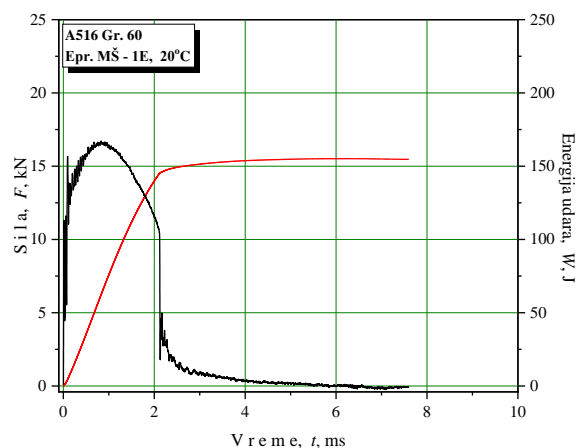
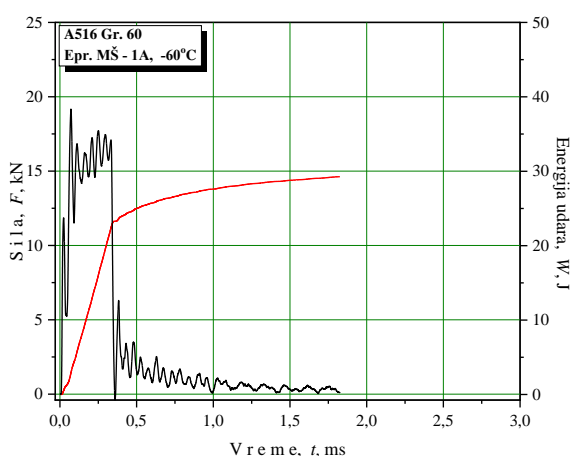
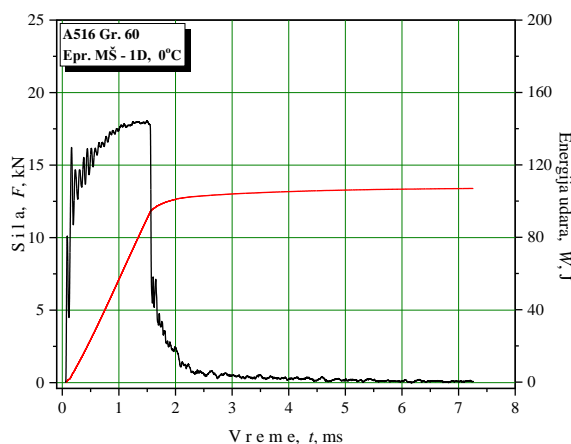
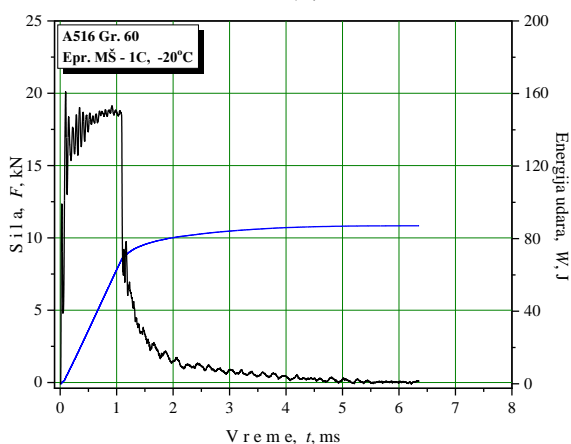
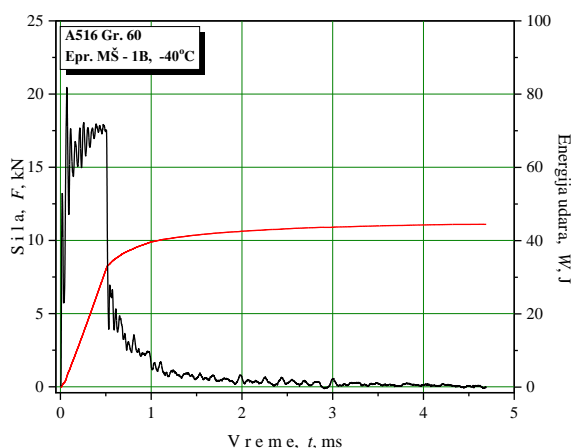


Figure 13. The WM results - force-time diagrams.



DISCUSSION

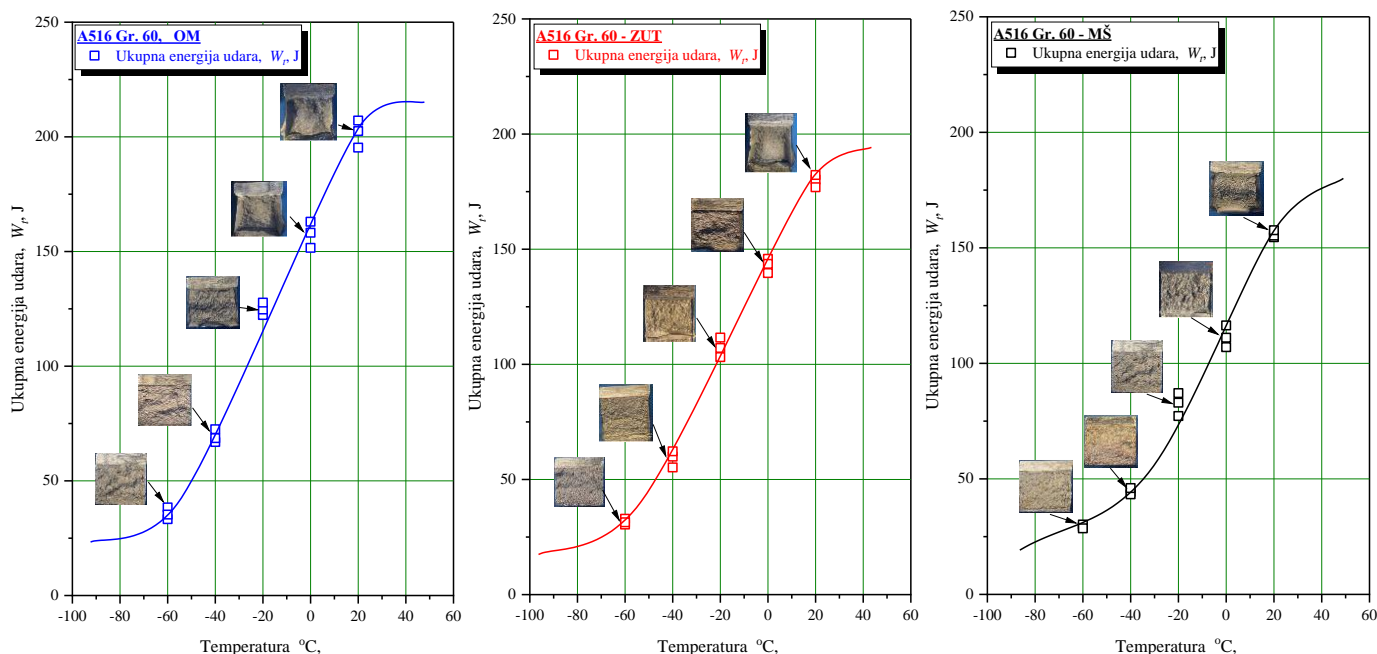
By analysing the obtained curves, it can be seen that they exhibit similar dependence at same temperatures, with only differences being observed in terms of maximal force, F_{\max} , deflection s , and total impact energy W_i . Dependence of total impact energy, W_i , from temperature and the location of the notch is shown in Fig. 14. It is well known that the total impact energy W_i depends on:

- location of notch in terms of welded joint region,
- testing temperature.

By analysing the effect of notch location on total impact energy (Tables 4-6), it can be concluded that the heterogeneity between the microstructures of BM and WM, results in different mechanical properties and considerably affects total impact energy values. Highest total impact energy values are observed in the BM, whereas specimens with the notch in HAZ had slightly lower values and the lowest ones were obtained for specimens with the notch in the WM.

However, the highest effect on obtained values of total impact energy and its components (crack initiation and propagation energy), as well as on the failure mechanisms and appearance of fracture surfaces was due to test temperature. Since A516 Gr. 60 steel has a body-centred cubic structure, the effect of temperature is evident. Lowering of temperature favours the initiation of a brittle state and is particularly prominent for this type of steels and welded joints, as typical heterogeneous structures.

Total impact energy, W_i , decreases as the temperature lowers, in a successive manner from room temperature to -60°C for all welded joint zones (BM - HAZ - WM). Influence of test temperature is most significant for specimens with the notch in the WM, slightly less for HAZ, and the lowest for the BM. More prominent influence of test temperature is closely related to the heterogeneity of WM and HAZ. Weld metal represents previously melted filler material (electrode) and is characterised by a cast structure. Heat affected zone represents the most heterogeneous welded joint region, due to the effect of weld metal melting has on the base metal. In this particular case, due to well defined welding parameters, structural transformation of the BM was somewhat low, hence, the obtained total impact energy values are very close to the BM itself.

Figure 14. Dependence of total impact energy W_t on temperature.

Total impact energy values obtained for specimens with a V-2 notch in the BM had an average of 202 J. With a decrease in temperature, these values also drop. At 0 °C, the mean total impact energy for these specimens is 167 J. Further decrease in temperature (-20 °C) resulted in an average of 125 J, whereas test temperature of -40 °C caused the total impact energy to decrease to an average of 69 J. Finally, at -60 °C the mean value of total impact energy was around 36 J.

For specimens with the V-2 notch in HAZ, overall values of total impact energy were slightly lower compared to the BM specimens, with an approximate difference of 10 %. At room temperature, their mean value was 179 J, whereas at 0 °C, this value was 143 J. Average value of total impact energy at -20 °C was lowered to 107 J, and at -40 °C it was around 59 J. Finally, at -60 °C the mean value of total impact energy was around 32 J.

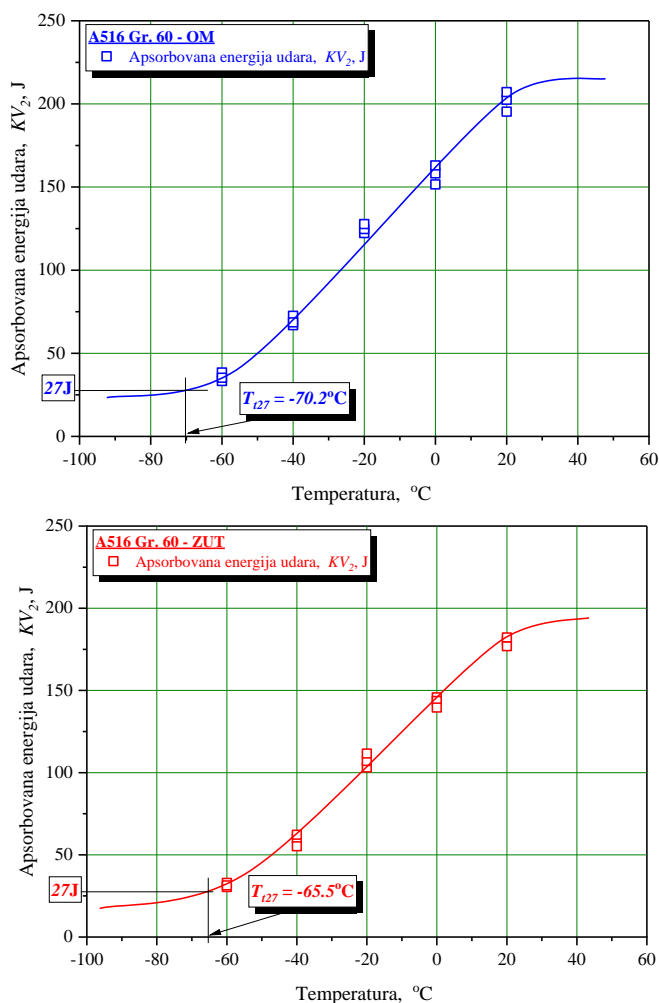
As previously mentioned, the temperature effect on total impact energy was most prominent for test specimens with V-2 notch in the WM. At room temperature, total impact energy mean value was 156 J, and at 0 °C it was 111 J. Further decrease in temperature resulted in mean total impact energy value of 82 J for -20 °C test temperature and 45 J for -40 °C. Finally, at -60 °C the mean value was around 29 J.

Annex D from standard SRPS EN ISO 148-1:2016, /16/, defines four criteria that can be used to determine the transition temperature. The most commonly used is the 27 J criterion, i.e., temperature at which impact energy equals 27 J. Values of transition temperatures for all three welded joint regions are given in Table 7.

Table 7. Transition temperatures for a welded joint.

Notch location	Transition temperature, T_i , (°C), at 27 J
BM	-70.2
HAZ	-65.5
WM	-61.6

Transition temperature is determined using the absorbed impact energy (KV)-temperature (T) curve, as shown in Fig. 15 for the BM, WM, and HAZ.



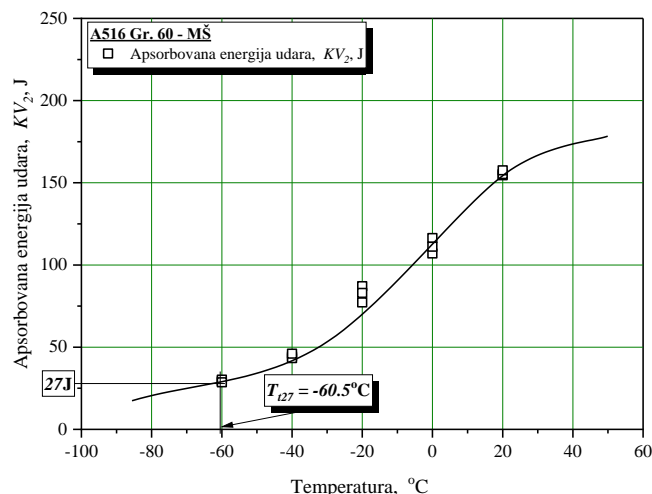


Figure 15. Total impact energy vs. temperature (BM, HAZ, WM).

Crack propagation energy share for BM specimens at room temperature is around 73 % of total impact energy. This share decreases with temperature, and is 59 % at 0 °C, 53 % at -20 °C, around 28 % at -40 °C, and only 24 % of total impact energy at -60 °C.

In the case of the HAZ, crack propagation energy share at room temperature is around 67% of total impact energy. This decreases to 54% for 0 °C and continues to decrease at lower temperatures. At -20°C, crack propagation energy share is 51%, at -40°C it is around 24% and at -60°C it represents 13% of total impact energy.

As for specimens with the notch in the WM, room temperature tests had shown that the crack propagation energy share is around 58% of total impact energy, whereas at 0°C it is 48%. At -20°C test temperature, this share is around 40%, at -40°C it is 22%, and at -60°C it decreases to 11% of total impact energy.

CONCLUSIONS

The goal of this paper is to determine the behaviour of A516 Gr. 60 steel under impact load for each welded joint zone (BM, HAZ and WM) tested at different temperatures.

Based on the obtained results, it is concluded that the specimens with a notch in the BM had shown the best behaviour under impact load, with highest impact energy values, and biggest share of crack propagation energy. Specimens with the notch in the WM had the lowest values, but all of the obtained results are still acceptable for each welded joint region, even at temperatures as low as -60 °C. This is further confirmed after determining the transition temperatures for each welded joint region, all of which are below -60 °C.

REFERENCES

- Jovanović, M., Čamagić, I., Sedmak, S., et al. (2022), *The effect of material heterogeneity and temperature on impact toughness and fracture resistance of SA-387 Gr.91 welded joints*, Materials, 15(5): 1854. doi: 10.3390/ma15051854
- Jovanović, M., Čamagić, I., Sedmak, S., et al. (2022), *Effect of material heterogeneity and testing temperature on fatigue behaviour of Cr-Mo steel welded joints*, Eng. Fail. Anal. 141: 106542. doi: 10.1016/j.eng-failanal.2022.106542

- Vojvodic Tuma, J., Sedmak, A. (2004), *Analysis of the unstable fracture behaviour of a high strength low alloy steel weldment*, Eng. Fract. Mech. 71(9-10): 1435-1451. doi: 10.1016/S0013-7944(03)00166-8
- Mastilović, S., Djordjević, B., Sedmak, A., Kirin, S. (2023), *Size effect assessment of K_{Jc} experimental data using the two-step-scaling method*, Struct. Integr. Life, 23(2): 105-110.
- Djordjevic, B., Mastilovic, S., Sedmak, A., et al. (2023), *Ductile-to-brittle transition of ferritic steels: A historical sketch and some recent trends*, Eng. Fract. Mech. 293: 109716. doi: 10.1016/j.engfractmech.2023.109716
- Mastilovic, S., Djordjevic, B., Sedmak, A., Kirin, S. (2024), *Data-driven prediction of fracture toughness size effect in ductile-to-brittle transition using Two-Step-Scaling procedure*, Eng. Fract. Mech. 307: 110339. doi: 10.1016/j.engfractmech.2024.110339
- Đorđević, B., Sedmak, A., Petrovski, B., et al. (2020), *Load and deformation effects on brittle fracture of ferritic steel 20MnMoNi55 in temperature transition region*, Struct. Integr. Life, 20(2): 184-189.
- <https://cms.sij.si/storage/587/SIQUAL-catalogue-v2024-20.6.2024.pdf> (last accessed Nov. 1, 2024)
- ASTM A516/A516M-10, Standard Specification for Pressure Vessel Plates, Carbon Steel, for Moderate- and Lower-Temperature Service, 2015. doi: 10.1520/A0516_A0516M-10R15
- Nanstad, R.K., Swain, R.L., Berggren, R.G. (1990), *Influence of thermal conditioning media on Charpy specimen test temperature*, Charpy Impact Test: Factors and Variable, ASTM STP 1072, ASTM, p. 195, 1990.
- SRPS EN ISO 9016:2022. Destructive tests on welds in metallic materials - Impact tests - Test specimen location, notch orientation and examination.
- SRPS EN ISO 14556:2023. Metallic materials - Charpy V-notch pendulum impact test - Instrumented test method.
- Sedmak, S., Radović, A., Grabulov, V. (2002), *The analysis of crack initiation/propagation energy ratio in steel at different temperatures*, Struct. Integr. Life, 2(1-2): 5-10.
- Jovanović, M., Čamagić, I., Sedmak, S.A., et al. (2020), *Crack initiation and propagation resistance of HSLA steel welded joint constituents*, Struct. Integr. Life, 20(1): 11-14.
- Jovanović, M., Čamagić, I., Sedmak, A., et al. (2021), *Analysis of SA 387 Gr. 91 welded joints crack resistance under static and impact load*, Procedia Struct. Integr. 31: 38-44. doi: 10.1016/j.prostr.2021.03.008
- SRPS EN ISO 148-1:2017. Metallic materials - Charpy pendulum impact test - Part 1: Test method - ISO 148-1:2016.

© 2024 The Author. Structural Integrity and Life, Published by DIVK (The Society for Structural Integrity and Life 'Prof. Dr Stojan Sedmak') (<http://divk.inovacionicentar.rs/ivk/home.html>). This is an open access article distributed under the terms and conditions of the [Creative Commons Attribution-NonCommercial-NoDerivatives 4.0 International License](#)